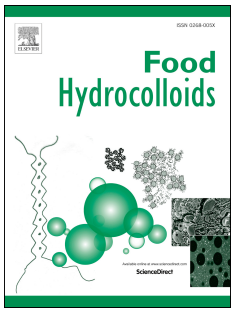

Incorporation of cinnamon essential oil-loaded Pickering emulsion for improving antimicrobial properties and control release of chitosan/gelatin films

Simin Fan, Debao Wang, Xiangyuan Wen, Xin Li, Fei Fang, Aurore Richel, Naiyu Xiao, Marie-Laure Fauconnier, Chengli Hou, Dequan Zhang

PII: S0268-005X(22)00958-4

DOI: https://doi.org/10.1016/j.foodhyd.2022.108438

Reference: FOOHYD 108438

To appear in: *Food Hydrocolloids*

Received Date: 21 November 2022

Revised Date: 20 December 2022

Accepted Date: 24 December 2022

Please cite this article as: Fan, S., Wang, D., Wen, X., Li, X., Fang, F., Richel, A., Xiao, N., Fauconnier, M.-L., Hou, C., Zhang, D., Incorporation of cinnamon essential oil-loaded Pickering emulsion for improving antimicrobial properties and control release of chitosan/gelatin films, *Food Hydrocolloids* (2023), doi: https://doi.org/10.1016/j.foodhyd.2022.108438.

Credit author statement

Simin Fan: Investigation; Data curation; Formal analysis; Writing - original draft.

Debao Wang: Methodology; Validation; Writing - review & editing.

Xiangyuan Wen: Resources; Data curation.

Xin Li: Validation; Visualization.

Fei Fang: Resources; Project administration.

Aurore Richel: Writing - review & editing, Supervision.

Naiyu Xiao: Writing - review & editing, Supervision.

Chengli Hou: Conceptualization; Writing - review & editing; Supervision.

Dequan Zhang: Conceptualization; Writing - review & editing; Funding acquisition; Supervision.

Graphical abstract

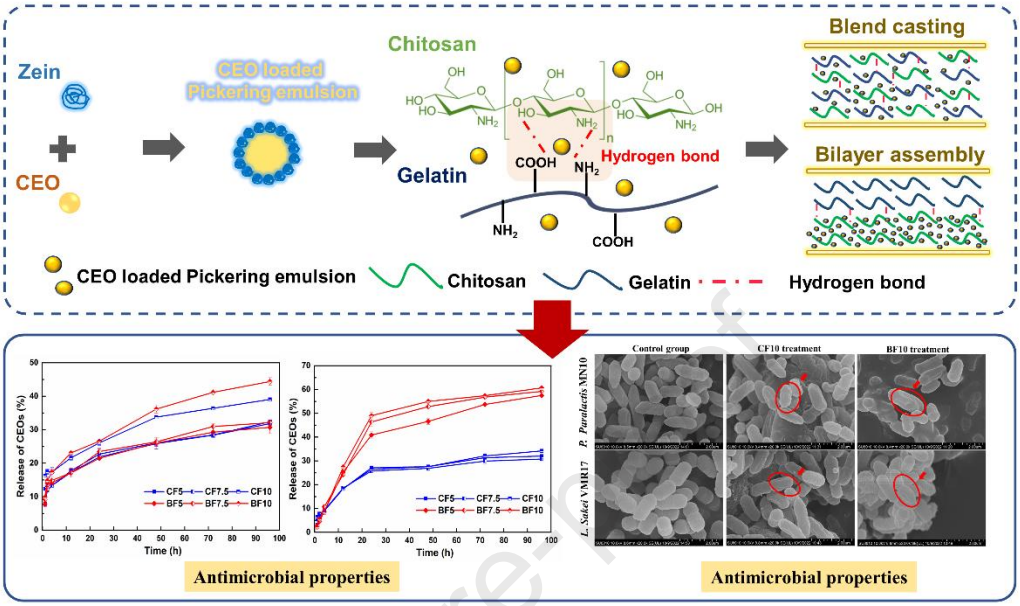

Incorporation of cinnamon essential oil-loaded Pickering emulsion for improving antimicrobial properties and control release of chitosan/gelatin films

Simin Fan[a,b], Debao Wang[a], Xiangyuan Wen[a], Xin Li[a], Fei Fang[a], Aurore Richel[b], Naiyu Xiao[c], Marie-Laure Fauconnier[d], Chengli Hou[a,*], Dequan Zhang[a,*]

[a] Institute of Food Science and Technology, Chinese Academy of Agricultural Sciences, Key Laboratory of Agro-products Processing, Ministry of Agriculture and Rural Affairs, Beijing 100193, China

[b] Laboratory of Biomass and Green Technologies, Gembloux Agro-Bio Tech, University of Liege, Passage des déportés 2, B-5030 Gembloux, Belgium

[c] College of Light Industry and Food Science, Zhongkai University of Agriculture and Engineering, Guangzhou 510225 Guangdong, China

[d] Laboratory of Chemistry of Natural Molecules, Gembloux Agro-Bio Tech, University of Liége, Passage des déportés 2, B-5030 Gembloux, Belgium

***Corresponding author: Dequan Zhang**

Institute of Food Science and Technology, Chinese Academy of Agricultural Sciences, Beijing 100193, China

E-mail address: dequan_zhang0118@126.com

***Corresponding author: Chengli Hou**

Institute of Food Science and Technology, Chinese Academy of Agricultural Sciences, Beijing 100193, China

22 E-mail address: houchengli@caas.cn

Abstract:

In this research, cinnamon essential oil (CEO) loaded Pickering emulsion was incorporated into chitosan (CS)/gelatin (GEL) complex films. These antimicrobial functionalizations of biobased packaging films containing different contents (5, 7.5, and 10 mL) of CEO-loaded Pickering emulsion were evaluated on the microstructure, physicochemical, mechanical, barrier and antimicrobial properties. CEO-loaded Pickering emulsion was herein prepared with zein nanoparticles as a stabilizer showed an average size of 113.37 nm and exhibited excellent physical stability. Fourier transform infrared spectroscopy (FTIR) and wide-angle X-ray scattering (WAXS) analyses revealed that the CEO-loaded Pickering emulsion showed compatibility with CS/GEL matrix. Not only mechanical properties but also barrier properties of the prepared films were significantly improved ($P < 0.05$) by incorporating CEO-loaded Pickering emulsion. Furthermore, incorporating CEO-loaded Pickering emulsion with CS/GEL led to the formation of high antimicrobial films against *Pseudomonad paralactis* MN10 and *Lactobacillus sakei* VMR17 with slow-release behavior of CEO. These results suggested that Pickering emulsion is a promising antimicrobial agent delivery system for biopolymer based active packaging, notably for the conception of novel active packaging biobased polymers.

Keywords: Antimicrobial packaging; Pickering emulsion; Cinnamon essential oil; Chitosan/gelatin composite films; Control release

1. Introduction

Conventional plastics have significantly contributed to the development of the food packaging industry due to their functions in the containment, protection and distribution of food. Conventional plastics are synthetic materials by petroleum-based polymers, which bring serious problems in resource depletion, and environmental pollution due to their low biodegradability and poor recyclability (Chamas, et al., 2020). To overcome the threats associated with petroleum-based plastic packaging materials, the development of sustainable resources to exploit biodegradable and renewable packaging materials with eco-friendly features is being actively studied (Al-Maqtari et al., 2022; Garavand et al., 2020). Several biobased polymers, such as polysaccharides (cellulose, chitosan, etc.) or proteins (gelatins, zein, etc.) (Wang et al., 2021&2022), are currently being investigated as plastic viable alternatives, which get noticed because of their biodegradability and biocompatibility and good film-forming abilities (Jafarzadeh, et al., 2020).

Gelatin (GEL) is one of the most intriguing protein-based biopolymers, owing to its good film-forming capabilities and highly processable properties. However, pure GEL film has weaknesses of poor tensile strength and high moisture-sensitive that need to be resolved before perfect utilization (Dai et al., 2022). The incorporation of different matrices with complementary characteristics is considered as an enhancement strategy for characteristics of pure GEL film (Qiao et al., 2017). Chitosan (CS), as a positively charged polysaccharide, has been widely used in the preparation of film due to its strong

film-forming capacity and biocompatibility (Do et al., 2022). CS is considered a candidate for the enhancement of mechanical and physicochemical properties of pure GEL films (Roy & Rhim, 2021a). The synergistic effect is performed associated with electrostatic interactions between the negatively charged carboxyl group of GEL and the positively charged amino group of CS and strong hydrogen bond formation (Liu et al., 2022). Based on the broad range of molecular interactions, the layer-by-layer assembly method has gained interest (Zhao et al., 2020). Both blending and assembly provide alternative approaches for the preparation of CS and GEL films. Recent studies focus on exploring the antimicrobial function of CS/GEL complex films for the development and application of food active packaging films (Al-Maqtari et al., 2022; Uranga et al., 2019).

Essential oils (EOs), as natural bioactive compounds derived from plants, take over wide attention as antimicrobial agents in food active packaging films due to their safety and effective antimicrobial performance (Calo et al., 2015). Cinnamon essential oil (CEO), mainly contains cinnamaldehyde (> 70%) and (-)-α-pinene (> 10%), which have been confirmed that possess antimicrobial activities for bacteria and fungi (Yang et al., 2021; Zhang et al., 2019). However, the incorporation of EOs directly into biobased packaging films has some major challenges due to thermally sensitive and easy inactivation during the film-forming process (Hosseini, Ghaderi, & Gómez-Guillén, 2022). In addition, free EOs loaded bio-based films have a “dumping effect” of active compounds, which could result in limited effectiveness of active films during

applications (Zhang et al., 2022c). Thus, the encapsulation strategy is required to decrease bioactivity losses of EOs during food active packaging creation (Shao et al., 2021). Pickering emulsion, as known as a bioactive compounds delivery system, exhibits the protection of bioactive compounds and a controlled release. Recently, Pickering emulsion has received increasing interest in the encapsulation of EOs (Zhang et al., 2022c). Previous reports have proven the protection capability and controlled release of EOs loaded Pickering emulsion (Liu et al., 2019; Shen et al., 2021). Pickering emulsion is stabilized by amphiphilic colloidal particles that help to reduce the interfacial tension between water and oil phases and promote the formation of emulsion droplets (Wu et al., 2022). Particle wettability of the colloidal emulsion surface decides the adsorption properties and physical stability of the Pickering emulsion (Shao et al., 2019; Mwangi et al., 2020). For example, zein particles enhanced the physical stability of Pickering emulsion due to their hydrophobic and hydrophilic nature, which could enhance the attraction in stabilizer particles on droplets interface (Soltani &Madadlou, 2016). Moreover, the high stability Pickering emulsion may result in better performance of food active packaging because of the better dispersion characteristics in the film matrix. However, there is limited information reported on adding EOs loaded Pickering emulsion to CS/GEL composite films.

Therefore, the objective of this research was to develop CS/GEL composite film by incorporating CEO-loaded Pickering emulsion as an antimicrobial agent delivery system for active packaging applications. The structure, physical, mechanical and

barrier properties of CEO-loaded Pickering emulsion CS/GEL films were assessed. Furthermore, the release behavior and antimicrobial activity against spoilage bacteria of the films were investigated.

2. Materials and methods

2.1. Materials and reagents

Zein was purchased from Sigma-Aldrich (St. Louis, MO, USA). CS (CAS#:9012-76-4, MW of 50000) was purchased from Shanghai Macklin Biological Co., Ltd. (Shanghai, China). GEL (CAS#:9000-70-8, type A, bloom value of 300) and glycerol were procured from Yuanye Bio-Technology Co., Ltd. (Shanghai, China). CEO was purchased from Jiangxi Taicheng natural perfume Co., Ltd. (Ji'an, China). Absolute ethyl alcohol, acetic acid and other reagents were purchased from Sinopharm Chemical Reagent Co., Ltd (Beijing, China). Tryptic soy broth (TSB) medium and DeMan-Rogosa-Sharpe broth (MRS) medium were obtained from Beijing Land Bridge Technology Co., Ltd. (Beijing, China). All reagents used in this work are analytically pure. *Pseudomonad paralactis* MN10 (*P. paralactis* MN10) and *Lactobacillus sakei* VMR17 (*L. sakei* VMR17) were obtained from Meat Science and Nutrition Innovation Laboratory of the Institute of Food Science and Technology, Chinese Academy of Agricultural Sciences (Beijing, China).

2.2. Preparation of CEO-loaded Pickering emulsion

The preparation of CEO-loaded Pickering emulsion was referred to literature

(Mattice & Marangoni, 2020) with slight modifications. Firstly, zein dissolved in acetic acid aqueous solution (90%, v/v) to form zein stock solutions. Stock solutions were added to ultrapure water with homogenized by HR-500 high shear homogenizing emulsifiers (Shanghai Huxi Industry Co., Ltd, Shanghai, China) at speed of 12000 rpm for 5 min to form zein nanoparticles dispersion (1%, w/v). Next, CEO was added dropwise into zein nanoparticles dispersion to form CEO-loaded Pickering emulsion under homogenized at speed of 12000 rpm for 5 min. The final concentration of CEO in the Pickering emulsion system was 1% (v/v).

2.3. Characterization of CEO-loaded Pickering emulsion

2.3.1. Measurement of particle size, polydispersity index and Zeta potential

Particle size, polydispersity index (PDI), and Zeta potential of CEO-loaded Pickering emulsion were measured by Zetasizer Nano ZS (Malvern Instruments Inc., Malvern, UK). The CEO-loaded Pickering emulsion samples were diluted 100 times with ultrapure water before measurements. Particle size, PDI, and Zeta potential were measured three times for each sample, and average values were reported.

2.3.2. Turbiscan stability index

The physical stability of CEO-loaded Pickering emulsion was measured using a Turbiscan Lab Expert analyzer (Formulaction Inc., Toulouse, France). The entire height of the emulsion was scanned by pulsed near-infrared light (λ =880 nm). Meanwhile, two synchronous detectors receive the light passing through the sample at

147 angles of 180° (transmission) and 45° (backscattering). Only the backscattering light
148 was measured because the emulsions were opaque. The sample (20 mL) was placed in
149 the test tube and scanned every 1 h continuously for 24 h at 25 ℃.

150 *2.3.3. Confocal laser scanning microscopy*

151 Confocal laser scanning microscopy (CLSM, Leica TCS SP8, Leica microsystems
152 Inc., Wetzlar, Germany) was employed to observe the microstructure of CEO-loaded
153 Pickering emulsion. The samples were labeled with mixture dyes of Nile Red (0.1%,
154 w/v) and Nile Blue (0.1%, w/v) at a ratio of 1:1. 10 μL sample and 10 μL mixture dyes
155 were successively dropped onto the slide for lightproof staining. Images of CEO-
156 loaded Pickering emulsion were recorded by CLSM at excitation wavelengths of 488
157 nm and 633 nm.

158 *2.4. Fabrication of CEO-loaded Pickering emulsion/chitosan/gelatin films*

159 GEL was dissolved in ultrapure water in a water bath at 50 ℃ for 2 h to form a
160 GEL solution (2%, w/v), the 30% (w/w, based on the dry GEL weight) glycerol was
161 then added to the GEL solution to obtain the GEL film forming solutions. CS was
162 dissolved in acetic acid aqueous solution (1.5%, v/v) in a water bath at 50℃ for 2 h to
163 form CS solution (1.5%, w/v), the 30% (w/w, based on the dry CS weight) glycerol
164 was then added to the CS film forming solutions. Different amounts of the CEO-loaded
165 Pickering emulsion (5, 7.5, and 10 mL) were mixed with CS film-forming solutions to
166 form active film-forming solutions (AFFS), of which volume was a total of 30 mL.

In this work, two forms of the film were prepared. To prepare the blend casting film (CF), 30 mL AFFS mixed with GEL film-forming solutions (30 mL) were cast into a 150 mm diameter plastic plate and dried at 50 ℃ for 18 h. The CF with different contents (5, 7.5, and 10 mL) of CEO-loaded Pickering emulsion were named CF5, CF7.5 and CF10, respectively. To prepare the bilayer film (BF), a layer-by-layer assembly method was employed. Briefly, GEL film forming solutions (30 mL) were poured into 150 mm diameter plastic plate and dried at 50℃ for 6 h to form the GEL layer firstly, then 30 mL AFFS were poured onto the GEL layer and dried for 12h to form the second layer. The BF with different contents (5, 7.5, and 10 mL) of CEO-loaded Pickering emulsion were represented as BF5, BF7.5 and BF10. All prepared films were conditioned for 48 h at 25℃ and 50% relative humidity (RH) before further measurements.

2.5. Characterization of Pickering emulsion/chitosan/gelatin films

2.5.1. Scanning electron microscope

Surface and cross-section structure of prepared films were observed by scanning electron microscope (SEM, SU 1510, Hitachi, Japan). Before scanning, the film samples were frozen in liquid nitrogen to obtain cross section, and then plated by a vacuum sputter coater (Bal-Tec AG, Blazers, Liechtenstein).

2.5.2. Fourier transform infrared spectroscopy

Infrared spectra of films were generated by Fourier transform infrared

187 spectroscopy (FTIR, Tensor 27, Bruker) in the range of 4000-400 cm^{-1} resolution after
188 32 scans. Prior to the measurement, a background spectrum was measured, and all
189 measures were performed in triplicate and the presentative one was provided.

190 *2.5.3. Wide-angle X-ray scattering*

191 Structural characterization of films was carried out through the wide-angle X-ray
192 scattering (WAXS) analyses on Anton Paar SAXS point 2.0 system (Anton Paar Ltd.,
193 Austria) using Cu Kα radiation as X-ray source (wavelength=1.5418 Å). The distance
194 between the film sample and the source was 78 mm. All data were deducted
195 background and smeared, and normalized before further analysis.

196 *2.5.4. Thickness and mechanical properties*

197 The thickness of the films was measured by using an MDC-25SX micrometer
198 caliper (Mitutoyo Corporation, Takatsu-ku, Kawasaki, Japan). The average thickness
199 was calculated through five random place measurement values. According to the
200 previous report (Hua et al., 2021), tensile strength (TS) and elongation at break (EAB)
201 of films were investigated by the texture analyzer (TA-XTPlus, Stable Micro System
202 Co., Ltd., UK). Firstly, the films were cut into 80 mm × 15 mm rectangles. The initial
203 grip separation of the fixture was 50 mm and the stretching speed was 50 mm/min.

204 *2.5.5. UV visible light transmittances*

205 The light transmittances of films were measured with a UV spectrophotometer
206 (UV-6000PC, Shanghai Metash Instruments Co., Ltd., Shanghai, China) at the range

of 200 to 800 nm. The film sample was cut into strips with 40 mm × 10 mm and then placed in the sample tank for analysis.

2.5.6. Thermogravimetric analysis

Thermogravimetric analysis (TGA) of films was measured using a thermogravimetric analyzer (Pyris Diamond TG/DTA, PerkinElmer Inc., New Castle, DE, USA). 4.0 g of the film sample was sealed in aluminum pans and was heated from 30 to 550 ℃ at a temperature programming of 10 ℃/min.

2.5.7. Water content and water solubility

The water content (WC) and water solubility (WS) of films were determined by the method of Ahammed et al. (2021) with simple modifications. The film sample was cut to a 30 mm × 30 mm square and weighed to determine the initial weight (M_0). Then the film sample was dried at 105 °C for 24 h, then weighed and recorded as (M_1). The MC of films was calculated according to the formula (1):

$$MC\ (\%) = \frac{(M0 - M1)}{M0} \times 100 \quad (1)$$

The dried sample was immersed into a beaker with 20 mL of ultrapure water and stirred for 24 h at 25 °C. The undissolved part of the film was taken out and dried at 105℃ for 24 h and weighed as (M_2). The MS of films was calculated according to the formula (2):

$$MS(\%) = \frac{(M1 - M2)}{M1} \times 100 \quad (2)$$

2.5.8. Water vapor permeability and oxygen permeability

The water vapor permeability (WVP) of the film was measured according to the previous method of Liu et al. (2020), with slight modifications. The beaker (diameter of 55 mm) with 10 g of anhydrous calcium chloride was sealed by film sample. Then the beaker was kept in the environmental condition at 25 °C and 75% RH. The beaker was checked every 12 h for 2 d to determine the weight loss. The WVP was calculated according to equation (3).

$$WVP\ (g/(m\ s\ Pa)) = \frac{\Delta S \times d}{t \times A \times \Delta \mathrm{P}} \quad (3)$$

where ΔS was the weight loss of the beaker (g), d was the thickness of the film (mm). t was the measuring time (s), A was the area of the mouth of the beaker (mm^2), ΔP was the pressure difference inside and outside the beaker.

Oxygen permeability (OP) was determined based on the report of Wang et al. (2018). Briefly, the beaker (diameter of 55 mm) with 10 g of deoxidizer was sealed by film sample. Then the beaker was kept in the environmental condition at 25 °C and 75% RH. The beaker was checked every 12 h for 2 d to determine the weight loss. The OP was calculated as equation (4).

$$OP\ (\mathrm{g/(m\ s\ Pa)}) = \frac{\Delta \mathrm{M} \times d}{t \times A \times \Delta \mathrm{P}} \quad (4)$$

where ΔM was the weight loss of the beaker (g), d was the thickness of the film (mm). t was the measuring time (s), A was the area of the mouth of the beaker (mm^2), ΔP was the pressure difference inside and outside the beaker.

2.6. Release behavior

The release of the CEO from the films was assessed in food simulant according

to the method of Zhang et al. (2022b) with slight modifications. 50% ethanol solution and 95% ethanol solution were selected as a simulant of semi-fatty foodstuffs and fatty foodstuffs, respectively. Briefly, the film sample was cut into a 30 mm× 30 mm square and placed in a beaker with 50 mL of food simulant solution, then the beaker was kept at 25℃ for 96 h. Simulant samples were taken at predetermined time intervals (0, 1, 2, 4, 6, 12, 24, 48, 64, and 96 h). The amount of CEO release from the film was measured at 287 nm by UV–Vis spectrophotometer. The release percentage of the CEO from the film was calculated according to equation (5):

$$Releases\ percentage\ (\%) = \frac{Mt}{M} \times 100\ (\%) \quad (5)$$

where Mt was the amount of CEO released from the film at n^{th} t (h), and M was the initial concentration of CEO in the films.

2.7. Antimicrobial activity

2.7.1. Growth profiles of bacteria

The antimicrobial ability of films to *P. paralactis* MN10 and *L. sakei* VMR17 were evaluated according to the method of Xu et al. (2020). Briefly, a film sample (150.0 ± 0.5 mg) was added into sterilized centrifuge tube with 20 mL liquid medium (TSB for *P. paralactis* MN10 and MRS for *L. sakei* VMR17), and 100 μL of bacterial suspensions (10^7 CFU/mL) was inoculated to the liquid medium. The centrifuge tubes were incubated at 28 °C for 24 h with sustained shaking. Samples were removed at predetermined time intervals for optical density measurement at 600 nm by Spark multimode microplate reader (Tecan Inc., Switzerland).

2.7.2. Morphology of bacteria observed by SEM

The microstructure of *P. paralactis* MN10 and *L. sakei* VMR17 were observed with a scanning electron microscope (SU 1510, Hitachi, Japan). Under the same conditions as in section 2.7.1, the bacteria were cultured with film in a liquid medium for 4 h. The bacteria sediment was collected by centrifugated at 4 ℃ with the speed of 8000 g, and was fixed with 2.5 wt% glutaraldehyde overnight. Then, the fixed bacteria were gradient dehydrated with different concentrations of ethanol solution (in turn 30%, 50%, 70%, 90%, and 100%, v/v). Finally, the 100% ethanol was replaced with 100 % tert-butanol. The dehydrated bacteria were dried with critical point drying (Leica model EM CPD300, Austria). Prior to scanning, the bacteria samples were plated by a vacuum sputter coater.

2.8. Statistical analysis

The data were analyzed by SPSS 26.0 software (SPSS Inc., Chicago, IL, USA), and expressed by mean ± standard deviation. Analysis of variance (ANOVA) and Duncan's multiple tests at $P < 0.05$ were used to evaluate the significance of differences in means.

3. Results and discussion

3.1. Characterization of CEO-loaded Pickering emulsion

CEO-loaded Pickering emulsion was prepared with zein nanoparticles as stabilizer. The results of size distribution, physical stability, and morphology of CEO-

loaded Pickering emulsion were shown in Fig. 1. The average droplet size of CEO-loaded Pickering emulsion was 113.37 nm, and the main size distribution showed a single peak pattern (Fig. 1 (A)). The size distribution of the emulsion was an important parameter for its stability (Almasi, Azizi, & Amjadi, 2020). The average particle size of zein nanoparticles stabilized CEO-loaded Pickering emulsion was lower than that reported by Xu et al. (2020). They prepared zein colloidal particles stabilized clove essential oil Pickering emulsion (CP), the particle size of CP was in the range of 1.40~1.73 μm.

The Zeta potential and PDI value of CEO-loaded Pickering emulsion were + 67.27 mV and 0.29, respectively. Zeta potential measure the repulsive force or attraction between particles and oil phase, and PDI refer to the dispersibility of emulsion. The emulsion was considered as stability system when the absolute value of Zeta potential was above 30 mV (Niroula, Gamot, Ooi, & Dhital, 2021). An increase in Zeta potential promoted the dispersion and stabilization of emulsion. In the present manuscript, the zein was fully dissolved in glacial acetic acid to prepare colloid particles as a Pickering emulsion stabilizer. This operation makes zein colloid particles become protonated and highly unfolded, thus adsorption property is improved on the surface of Pickering emulsion (Mattice & Marangoni, 2020), which can prevent the formation of aggregation of emulsion. The smaller size and higher Zeta potential value of CEO-loaded Pickering emulsion were attributed to the highly plasticized and continuous network of zein nanoparticles (Mattice et al., 2020), possessing high

physical stability (Fig. 1 (B)). The TSI reflects the stability of the emulsion by recording the optical properties of the emulsion in real-time. The TSI value was negatively correlated with the Pickering emulsion stability (Zhao et al., 2023). A lower TSI implies a smaller variation in droplet concentration and a greater stable emulsion. The TSI value of the CEO-loaded Pickering emulsion was below 1.5 showing the emerging destabilization and high physical stability of the prepared emulsion (Jia et al., 2023). The morphology of CEO-loaded Pickering emulsion was visualized using CLSM and shown in Fig. 1 (C). As shown in Fig. 2 (C) (i), the droplets of CEO-loaded Pickering emulsion were approximately spherical shape. Fig.2 (C) (ii), (iii) and (iv) showed that the dispersed CEO droplet was surrounded by zein nanoparticles and had good dispersibility. These results indicated the potential of CEO-loaded Pickering emulsion for being an antimicrobial agent delivery system. Hence, the CEO-loaded Pickering emulsion was incorporated into CS/GEL for preparing antimicrobial packaging.

3.2. Characterization of blend casting and bilayer assembly Pickering emulsion chitosan/gelatin /films

3.2.1. SEM

The microstructural properties of CEO-loaded Pickering emulsion CS/GEL films with blend casting and bilayer assembly film systems were shown in Fig. 2. According to Fig. 2 (CF0 and BF0), the surface of CS/GEL films displayed compact and glossy,

indicating high compatibility between CS and GEL due to non-covalent interactions (Haghighi et al., 2019). However, the surface of films tended to a slight roughness by the incorporation of CEO-loaded Pickering emulsion. A similar SEM morphology was observed by Liu, et al. (2022) in CS films containing the cellulose nanocrystal-stabilized Pickering emulsions. Blend casting CEO-loaded Pickering emulsion CS/GEL film showed a tight structure in cross-section observation (Fig. 2 (CF10)). However, Fig. 2 (BF10) showed that the bilayer assembly CEO-loaded Pickering emulsion CS/GEL film presented a phenomenon of stacking, which could be as layer-by-layer assembly behavior during film forming (Zhang et al., 2019). In further observation of bilayer film, the CS side showed a roughness apparent obviously compared to the GEL side.

The microstructural properties affected the final physical, mechanical, barrier and optical properties of the films (Hosseini, Ghaderi, & Gómez-Guillén, 2021). GEL is an amphoteric electrolyte, the charged polar groups (–COOH, $–NH_2$, and –OH) in the structure chain could form an interaction with oppositely charged groups NH_3^+ of CS. Thus, both blend casting and bilayer assembly CEO-loaded Pickering emulsion CS/GEL films showed compatibility in film performance. And the structure of CS/GEL films was more tightly due to the filling action of CEO-loaded Pickering emulsion droplets. This phenomenon could be reflected in the mechanical and barrier properties of prepared films.

3.2.2. FTIR

FTIR was used to characterize the interactions between the chemical groups of films at the molecular level (Fig. 3 (A)). The characteristic functional groups of the CS, GEL, zein, and CEO mainly include hydroxyl, alkane, and amine. The vibrations and spectral positions could be altered when the main functional groups interacted with each other or with other groups (Zhang et al., 2019). The broad bands detected at 3222 and 3276 cm^{-1} were ascribed to the O-H and N-H stretching vibration of pure biopolymers (CS and GEL). However, the band of CS/GEL complex film distinctly moved to 3273 cm^{-1}, which was due to the hydrogen bond interactions between CS and GEL. With the addition of CEO-loaded Pickering emulsion, the intensity of absorption band at 3273 cm^{-1} gradually reduced. This was mainly due to the decrease of hydrogen bonding interactions between the -OH of GEL and the $-NH_2$ of CS, that caused by the decrease of CS content in prepared films. Such change in interactions verified the decline of the tensile strength of the prepared films in mechanical properties. In addition, the peaks at 2927 cm^{-1} were ascribed to the $-CH_2$ stretching vibrations of alkane groups. The peak at 1633 cm^{-1} and 1546 cm^{-1} were referred to the C-O stretching of amide-I and N-H bonds of amide-II, respectively. Bands at 1031 cm^{-1} were interpreted as the antisymmetric stretching of -C-O- in the glycosidic linkage, and vibration of the hexatomic ring ether (Li, et al., 2022). Overall, the peaks of the CEO-loaded Pickering emulsion CS/GEL films were like those of the CS/GEL films, except for minor changes in peak intensity. The above indicated incorporated CEO-loaded Pickering emulsion into CS/GEL films did not significantly change the chemical

structure of CS/GEL films.

3.2.3. WAXS

The crystalline structures of the CEO-loaded Pickering emulsion CS/GEL films were analyzed by wide-angle X-ray scattering and the results were shown in Fig. 3 (B). The WAXS patterns of CEO-loaded Pickering emulsion CS/GEL films displayed two diffraction peaks, and they were at around 9° and 20°, respectively, which can be assigned to its hydrated crystal and regular lattice, respectively (Chen et al., 2021). Notably, the peak intensity at around 9° of CEO-loaded Pickering emulsion CS/GEL films was increased, which could be explained as the reconstruction of intermolecular and intramolecular hydrogen bonds of films. In addition, the narrow peaks around 6° shown in patterns are ascribed to CS matrix in prepared films, which may be caused by the solution of chitosan solids in an acetic acid solution. Furthermore, Fig. 3 (B) showed that no other new sharp peaks appeared after adding the CEO-loaded Pickering emulsion with CS/GEL. These findings demonstrated that the presence of CEO-loaded Pickering emulsion did not change the crystal structure of the CS/GEL base matrix and could be evidence of the coexistence of the two phases of polymer matrix and CEO-loaded Pickering emulsion (Zhao et al., 2022).

3.2.4. Thickness and mechanical properties

The thickness of CEO-loaded Pickering emulsion CS/GEL films were shown in Table 1. The thickness of blend casting and bilayer assembly CS/GEL films were 66.61

(CF0) and 69.85 (BF0) μm, respectively. As the concentration of CEO-loaded Pickering emulsion increased, the thickness of CF10 and BF10 films were 74.81 and 78.03 μm, respectively. These results showed that the addition of CEO-loaded Pickering emulsion had a significant effect on the thickness of CS/CEL films. Mechanical properties were critical parameters for packaging films, which can affect their range of use and durability. The mechanical properties including TS and EAB of the CEO-loaded Pickering emulsion CS/GEL films were evaluated. As Table 1, the TS value of films gradually decreased with the increase of CEO-loaded Pickering emulsion, while the EAB of the CEO-loaded Pickering emulsion CS/GEL films significantly increased ($P < 0.05$). According to the result in FTIR and WASX above, the addition of CEO-loaded Pickering emulsion does not affect the chemical structure and crystal structure of the CS/GEL matrix. Thus, these changes in mechanical properties are mainly due to the filling effect that emulsion droplets cause on films, which leads to continuities in the biopolymer network. Liu et al. (2020) also found that the incorporation of Pickering emulsion did obviously change the mechanical properties of both TS and EAB of konjac glucomannan films, which were attributed to the deformability of filling lipid droplets in the films. However, Xu et al. (2020) attributed this result to the introduction of essential oils loaded with Pickering emulsion disrupting the ordered arrangement of the biopolymers matrix by interfering with the formation of inter- and/or intra-hydrogen bonds. In addition, TS and EAB values showed significant differences ($P < 0.05$) between CF and BF. TS value of CF showed

higher than BF, resulting in stronger and tougher films. This could be due to the intermolecular hydrogen bonds between the amino of CS and charged carboxyl of GEL. And the more condensed structure of CF than that of BF (Haghighi et al., 2019).

3.2.5. Light transmission

The appearance and light transmittance of CEO-loaded Pickering emulsion films were particularly important for food packaging films. As displayed in Fig. 4 (A) (CF0 and BF0), the appearance of CS/GEL films was flat and uniform, and the color of CS/GEL films appears a little yellow. With the addition of CEO-loaded Pickering emulsion, the color of CEO-loaded Pickering emulsion CS/GEL films presented whiteness and the lightness of films decreased. This observation can be explained by the milky white CEO-loaded Pickering emulsion equably integrated into CS/GEL films matrix.

Fig. 4 (B) showed the UV transmittance of the prepared films. It can be observed that with the addition of CEO-loaded Pickering emulsions, the UV transmittance of films present was reduced, suggesting an improved UV blocking ability. It was attributed to the phenolic compounds in CEO, which had UV absorption capacity and the differences in the refractive index of the continuous phase and the dispersed phase. A similar result was reported by Fasihi, et al. (2019) in carboxymethyl cellulose and polyvinyl alcohol films incorporated with rosemary essential oil-loaded Pickering emulsion. UV light is one of the main factors that accelerate the oxidation of unsaturated fatty acids (Jakubowska et al., 2023). Research had verified that the

addition of Pickering emulsion into a film can reduce the transmittance of light because of the dispersed droplets from the emulsion (Liu, et al., 2020). Thus, the food packaging films with great UV barrier properties were worth considering when applied.

3.2.6. Thermal properties

The TG and DTG curves of CEO-loaded Pickering emulsion CS/GEL films were shown in Fig. 4 (C) and Fig. 4 (D), respectively. The CEO-loaded Pickering emulsion CS/GEL films showed multiple steps of weight loss in TG and DTG curves. The initial weight change stage of films appeared at 120 ℃, which could be mainly due to the evaporation of free water. The second stage of weight loss was observed from 180 to 220 ℃. Weight loss of films at this stage was more likely attributed to the loss of structurally bound water, glycerol, and other low molecular weight compounds. The third range was observed from 260 to 330 ℃, which corresponded to a complex process involving the degradation of the polymer, especially of GEL (Roy & Rhim, 2020). A similar thermal degradation pattern was reported in the konjac glucomannan-based films incorporated with the Pickering emulsion of sunflower seed oil (Liu et al., 2020). As shown in Fig. 4 (D), the introduction of CEO-loaded Pickering emulsion improves the thermal stability of CS/GEL films. which agreed with the reported results in the literature (Zhao et al., 2022).

3.2.7. Water content and water solubility

The values of water related properties including WC and WS can be used to

454 evaluate the water sensitivity properties of the films, which could be greatly related to
455 physical properties. As shown in Table 1, the CS/GEL films displayed higher water
456 content, the values of CF0 and BF0 were 28.04 % and 32.97 %, respectively. However,
457 the WC values of films were decreased significantly with the CS/GEL films
458 incorporated with CEO-loaded Pickering emulsion ($P < 0.05$). These results were
459 mainly due to the hydrophobic CEO droplets wrapped in the emulsions, and the
460 interactions between CS/GEL and emulsions would replace partial CS/GEL and water
461 interactions. A similar result was reported by Shen et al. (2021), which found that the
462 pullulan-gelatin based films incorporated with clove essential oil-loaded Pickering
463 emulsion resulted in a decrease in WC. The WS of CS/GEL films displayed a higher
464 value (Table 1), 41.38 % and 35.86 % for CF0 and BF0, respectively. However, the
465 WS values of CEO-loaded Pickering emulsion incorporated with CS/GEL films
466 gradually decreased with the increase of CEO-loaded Pickering emulsion content.
467 These results were consistent with MC value described above due to the addition of
468 hydrophobic substances, which suggested that CEO-loaded Pickering emulsion could
469 contribute to improving the water hydrophobic of the CS/GEL films. Therefore, the
470 hydrophilic drawback of pure GEL could be overcome to some extent by the addition
471 of essential oil loaded Pickering emulsion.

472 *3.2.8. Barrier properties*

473 The barrier properties of films were evaluated using WVP and OP parameters.
474 WVP and OP of packaging films played critical roles in preventing moisture regain,

oxidation of food ingredients, and deterioration of food quality (Zhang, et al., 2019). As shown in Fig. 5. the WVP value of CS/GEL films were 1.36 and 1.76 $\times 10^{-10}$ g/(m s Pa) of CF0 and BF0, respectively. A significant difference in WVP value was found among films incorporated with different content of CEO-loaded Pickering emulsion ($P < 0.05$). The WVP value of CF10 and BF10 were 1.05 and 1.29 $\times 10^{-10}$ g/(m s Pa) respectively, which were lower than of gelatin/agar-based films integrated with clove essential oil loaded Pickering emulsion (0.62~0.71 $\times 10^{-9}$ g/(m s Pa)) (Roy & Rhim, 2021b). Water molecules can be absorbed into the films and interact with the free hydroxyl groups of CS. However, the hydrogen bonds between CS and GEL reduced the availability of hydrophilic groups. In addition, the droplets of hydrophobic CEO-loaded Pickering emulsion in CS/GEL films increased the tortuosity of the path of water vapor through films (Wang et al., 2018), and be shown in Fig. 5 (C).

The OP showed a similar trend of WVP in prepared films. The OP of CF0 and BF0 were 1.50 and 1.28 $\times 10^{-10}$ g/(m s Pa), respectively, and decreased as the addition of CEO-loaded Pickering emulsion. These results could be the addition of CEO-loaded Pickering emulsion reduced the mobility of polymer chain by forming uniform network structure between CS/GEL complex film forming matrix (Wang et al., 2021). Furthermore, as shown in Fig. 5 (C), the migration path of oxygen molecules was increased as same as water vapor. The results of WVP and OP, suggested that the incorporation with CEO-loaded Pickering emulsion into CS/GEL films could enhance the barrier properties of films.

3.3. Release behavior

50% ethanol solution (representing semi-fatty foodstuffs) and 95% ethanol solution (representing high-fatty foodstuffs) were selected as a simulant, respectively, to evaluate the CEO release behavior in films, and the results were shown in Fig. 6 (A1) and (A2). The release curve of CEO release in all films showed increasing trends until reached an equilibrium state during the test period, both in 50% ethanol solution and 95% ethanol solution. It could be due to the migration of the CEO from the CS/GEL film matrix to the simulant solution (Ahammed et al., 2021). In addition, the release behavior showed that the release rates were affected by the concentration of CEO in the film matrix, which suggested that the controlled release can be achieved by altering the amounts of CEO (Zhang et al., 2022a). However, a significant release rate was observed between CF and BF in 50% ethanol solution. This result was mainly due to the collapse of the bilayer assembly film structure in 50% ethanol solution. The 50% ethanol solution system had more water, causing the film to swell and even dissolve to some extent. In high hydrophilic system, the spatial network structure of the BF with weak intermolecular interaction was more likely to be destroyed, resulting in the increase of the release rate of CEO. This result implied that control release can be achieved by regulating the content of the CEO-loaded Pickering emulsion and the biopolymer film system.

3.4. Antimicrobial properties

Antibacterial properties of CEO-loaded Pickering emulsion CS/GEL were evaluated by determining the growth curve of the gram-negative pathogen (*P. paralactis* MN10) and gram-positive pathogen (*L. Sakei* VMR17), and observed morphology of bacteria by SEM. The details were shown in Fig.6 (B1) and (B2). The CEO-loaded Pickering emulsion CS/GEL films had a significant antimicrobial effect on *P. paralactis* MN10 and *L. Sakei* VMR17 Moreover, the CEO-loaded Pickering emulsion CS/GEL films seemed to inhibit effectively the growth of *L. Sakei* VMR17 than *P. paralactis* MN10, due partially to the differences in the cell wall structure of Gram-positive bacteria and Gram-negative bacteria (da Silva et al., 2022). These results can be ascribed to the interaction between the active compounds in CEO (cinnamaldehyde, phellandrene, and other phenolic substances) and the cell membrane of bacteria, leading to disruption of cell structure (Zhang et al., 2022b). To explore the mechanism of action of CEO-loaded Pickering emulsion CS/GEL against the *P. paralactis* MN10 and *L. Sakei* VMR17, the morphology of bacteria was observed by SEM (Fig. 6 (C)). In the control group, the *P. paralactis* MN10 exhibited a short rod shape and the *L. Sakei* VMR17 showed a two- long section shape, and the surfaces were smooth of *P. paralactis* MN10 and *L. Sakei* VMR17. However, under the treatments of CEO-loaded Pickering emulsion CS/GEL films, the cell adhesion aggregation and surface depression of *P. paralactis* MN10 and *L. Sakei* VMR17 were observed. Some reports had attributed the mechanism of EOs to inhibit microbial proliferation to their ability of penetration, which refer to penetrate through bacterial

cell membranes into the interior of the cell (Rao, Chen, & McClements, 2019). These results stated that the CEO-loaded Pickering emulsion CS/GEL films had the potential as an antimicrobial biobased food packaging material.

4. Conclusions

In this work, biobased antimicrobial packaging was successfully fabricated by incorporating CEO-loaded Pickering emulsion within CS/GEL film. The CEO-loaded Pickering emulsion has an average particle size of 113.37 nm and exhibited excellent physical stability. The microstructures of prepared films presented that the CEO-loaded Pickering emulsion was uniformly disputed in the films. FTIR and WAXS analyses revealed that the CEO-loaded Pickering emulsion showed compatibility with CS/GEL composite matrix, and thus improved the thermal stability of films. In addition, the mechanical properties of CS/GEL composite films were improved by the addition of CEO-loaded Pickering emulsion. Moreover, barrier properties for water vapor and oxygen were improved with the incorporation of CEO-loaded Pickering emulsion. Additionally, the CEO-loaded Pickering emulsion CS/GEL films had effective antimicrobial against spoilage bacteria *P. paralactis* MN10 and *L. Sakei* VMR17 under the controlled release of CEO of prepared films. In conclusion, the incorporation of CEO-loaded Pickering emulsion was a promising approach to enhance the antimicrobial properties of CS/GEL films. The beneficial properties in this work supported that CEO-loaded Pickering emulsion CS/GEL films had the potential capacity for food active packaging.

Credit author statement

Simin Fan: Investigation; Data curation; Formal analysis; Writing - original draft.

Debao Wang: Methodology; Validation; Writing - review & editing.

Xiangyuan Wen: Resources; Data curation.

Xin Li: Validation; Visualization.

Fei Fang: Resources; Project administration.

Aurore Richel: Writing - review & editing, Supervision.

Naiyu Xiao: Writing - review & editing.

Marie-Laure Fauconnier: Writing - review & editing.

Chengli Hou: Conceptualization; Writing - review & editing; Supervision.

Dequan Zhang: Conceptualization; Writing - review & editing; Funding acquisition; Supervision.

Acknowledgements

This work was financially supported by the National Key R&D Program of China (No. 2021YFD2100802). The authors thank Shanshan Liu, Tongjing Yan, Zhe Cheng, Yuqian Xu, Minghui Gu, Juan Chen, Jingyi Wei for their contributions on this work. The authors also appreciate the assistance by Mrs. Yanli Sun and Mrs. Ying Wang of Electron Microscope Center and Mrs. Chunhong Li of National Key Laboratory of Argo-products Processing, Institute of Food Science and Technology, Chinese Academy of Agricultural Science for their technical support.

References

Ahammed, S., Liu, F., Wu, J., Khin, M. N., Yokoyama, W. H., & Zhong, F. (2021). Effect of transglutaminase crosslinking on solubility property and mechanical strength of gelatin-zein composite films. *Food Hydrocolloids*, 116, 106649.

Almasi, H., Azizi, S., & Amjadi, S. (2020). Development and characterization of pectin films activated by nanoemulsion and Pickering emulsion stabilized marjoram (*Origanum majorana* L.) essential oil. *Food Hydrocolloids*, 99, 105338.

Al-Maqtari, Q. A., Al-Gheethi, A. A. S., Ghaleb, A. D. S., Mahdi, A. A., Al-Ansi, W., Noman, A. E., et al. (2022). Fabrication and characterization of chitosan/gelatin films loaded with microcapsules of Pulicaria jaubertii extract. *Food Hydrocolloids*, 129, 107624.

Calo, J. R., Crandall, P. G., O'Bryan, C. A., & Ricke, S. C. (2015). Essential oils as antimicrobials in food systems – A review. *Food Control*, 54, 111-119.

Chamas, A., Moon, H., Zheng, J., Qiu, Y., Tabassum, T., Jang, J. H., Abu-Omar, M., Scott, S. L., & Suh, S. (2020). Degradation rates of plastics in the environment. *ACS Sustainable Chemistry & Engineering*, 8(9), 3494-3511.

Chen, Y., Duan, Q., Yu, L., & Xie, F. (2021). Thermomechanically processed chitosan: gelatin films being transparent, mechanically robust and less hygroscopic. Carbohydrate Polymers, 272, 118522.

da Silva, B. D., do Rosário, D. K. A., Weitz, D. A., & Conte-Junior, C. A. (2022). Essential oil nanoemulsions: Properties, development, and application in meat and meat products. *Trends in Food Science & Technology*, 121, 1-13.

Dai, H., Peng, L., Wang, H., Feng, X., Ma, L., Chen, H., Yu, Y., Zhu, H., & Zhang, Y. (2022). Improved properties of gelatin films involving transglutaminase cross-linking and ethanol dehydration: The self-assembly role of chitosan and montmorillonite. *Food Hydrocolloids*, 132, 107870.

Do, N. H. N., Truong, Q. T., Le, P. K., & Ha, A. C. (2022). Recent developments in chitosan hydrogels carrying natural bioactive compounds. *Carbohydrate Polymers*, 294, 119726.

Fasihi, H., Noshirvani, N., Hashemi, M., Fazilati, M., Salavati, H., & Coma, V. (2019). Antioxidant and antimicrobial properties of carbohydrate-based films enriched with cinnamon essential oil by Pickering emulsion method. *Food Packaging and Shelf Life*, 19, 147-154.

Garavand, F., Cacciotti, I., Vahedikia, N., Rehman, A., Tarhan, O., ¨ Akbari-Alavijeh, S., et al. (2020). A comprehensive review on the nanocomposites loaded with chitosan nanoparticles for food packaging. *Critical Reviews in Food Science and Nutrition*, 62, 1383-1416.

Haghighi, H., De Leo, R., Bedin, E., Pfeifer, F., Siesler, H. W., & Pulvirenti, A. (2019). Comparative analysis of blend and bilayer films based on chitosan and gelatin enriched with LAE (lauroyl arginate ethyl) with antimicrobial activity for food packaging applications. *Food Packaging and Shelf Life*, 19, 31-39.

Hosseini, S. F., Ghaderi, J., & Gómez-Guillén, M. C. (2022). Tailoring physico-mechanical and antimicrobial/antioxidant properties of biopolymeric films by cinnamaldehyde-loaded chitosan nanoparticles and their application in packaging of fresh rainbow trout fillets. *Food Hydrocolloids*, 124, 107249.

Hua, L., Deng, J., Wang, Z., Wang, Y., Chen, B., Ma, Y., Li, X., & Xu, B. (2021). Improving the functionality of chitosan-based packaging films by crosslinking with nanoencapsulated clove essential oil. *International Journal of Biological Macromolecules*, 192, 627-634.

Jafarzadeh, S., Jafari, S. M., Salehabadi, A., Nafchi, A. M., Uthaya Kumar, U. S., & Khalil, H. P. S. A. (2020). Biodegradable green packaging with antimicrobial functions based on the bioactive compounds from tropical plants and their by-products. *Trends in Food Science & Technology*, 100, 262-277.

Jakubowska, E., Gierszewska, M., Szydłowska-Czerniak, A., Nowaczyk, J., & Olewnik-Kruszkowska, E. (2023). Development and characterization of active packaging films based on chitosan, plasticizer, and quercetin for repassed oil storage. *Food Chemistry*, 399, 133934.

Jia, Y., Dang, M., Khalifa, I., Zhang, Y., Huang, Y., Li, K., & Li, C. (2023). Persimmon tannin can enhance the emulsifying properties of persimmon pectin via promoting the network and forming a honeycomb-structure. *Food Hydrocolloids*, 135, 108157.

Li, H., Wu, C., Yin, Z., Wu, J., Zhu, L., Gao, M., & Zhan, X. (2022a). Emulsifying properties and bioavailability of clove essential oil Pickering emulsions stabilized by octadecylaminated carboxymethyl curdlan. *International Journal of Biological Macromolecules*, 216, 629-642.

Liu, J., Song, F., Chen, R., Deng, G., Chao, Y., Yang, Z., Wu, H., Bai, M., Zhang, P., & Hu, Y. (2022). Effect of cellulose nanocrystal-stabilized cinnamon essential oil Pickering emulsions on structure and properties of chitosan composite films. *Carbohydrate Polymers*, 275, 118704.

Liu, Q., Wang, W., Qi, J., Huang, Q., & Xiao, J. (2019). Oregano essential oil loaded soybean polysaccharide films: Effect of Pickering type immobilization on physical and antimicrobial properties. *Food Hydrocolloids*, 87, 165-172.

Liu, Y., Wang, R., Wang, D., Sun, Z., Liu, F., Zhang, D., & Wang, D. (2022). Development of a food packaging antibacterial hydrogel based on gelatin, chitosan, and 3-phenyllactic acid for the shelf-life extension of chilled chicken. *Food Hydrocolloids*, 127, 107546.

Liu, Z., Lin, D., Shen, R., & Yang, X. (2020). Characterizations of novel konjac glucomannan emulsion films incorporated with high internal phase Pickering emulsions. *Food Hydrocolloids*, 109, 106088.

Mwangi, W. W., Lim, H. P., Low, L. E., Tey, B. T., & Chan, E. S. (2020). Food-grade Pickering emulsions for encapsulation and delivery of bioactives. *Trends in Food Science & Technology*, 100, 320-332.

Mattice, K. D., & Marangoni, A. G. (2020). Functionalizing zein through antisolvent

precipitation from ethanol or aetic acid. *Food Chemistry*, 313, 126127.
Niroula, A., Gamot, T. D., Ooi, C. W., & Dhital, S. (2021). Biomolecule-based pickering food emulsions: Intrinsic components of food matrix, recent trends and prospects. *Food Hydrocolloids*, 112, 106303.
Qiao, C., Ma, X., Zhang, J., & Yao, J. (2017). Molecular interactions in gelatin/chitosan composite films. *Food Chemistry*, 235, 45-50.
Rao, J., Chen, B., & McClements, D. J. (2019). Improving the efficacy of essential oils as antimicrobials in foods: mechanisms of action. *Annual Review of Food Science and Technology*, 10(1), 365-387.
Roy, S., & Rhim, J.-W. (2020). Preparation of antimicrobial and antioxidant gelatin/curcumin composite films for active food packaging application. *Colloids and Surfaces B: Biointerfaces*, 188, 110761.
Roy, S., & Rhim, J.-W. (2021a). Fabrication of bioactive binary composite film based on gelatin/chitosan incorporated with cinnamon essential oil and rutin. *Colloids and Surfaces B: Biointerfaces*, 204, 111830.
Roy, S., & Rhim, J.-W. (2021b). Gelatin/agar-based functional film integrated with Pickering emulsion of clove essential oil stabilized with nanocellulose for active packaging applications. *Colloids and Surfaces A: Physicochemical and Engineering Aspects*, 627, 127220.
Shao, P., Feng, J., Sun, P., & Ritzoulis, C. (2019). Improved emulsion stability and resveratrol encapsulation by whey protein/gum arabic interaction at oil-water interface. *International Journal of Biological Macromolecules*, 133, 466-472.
Shao, P., Yu, J., Chen, H., & Gao, H. (2021). Development of microcapsule bioactive paper loaded with cinnamon essential oil to improve the quality of edible fungi. *Food Packaging and Shelf Life*, 27, 100617.
Shen, Y., Ni, Z. J., Thakur, K., Zhang, J.G., Hu, F., & Wei, Z. J. (2021). Preparation and characterization of clove essential oil loaded nanoemulsion and pickering emulsion activated pullulan-gelatin based edible film. *International Journal of Biological Macromolecules*, 181, 528-539.
Soltani, S., & Madadlou, A. (2016). Two-step sequential cross-linking of sugar beet pectin for transforming zein nanoparticle-based Pickering emulsions to emulgels. *Carbohydrate Polymers*, 136, 738-743.
Uranga, J., Puertas, A. I., Etxabide, A., Dueñas, M. T., Guerrero, P., & de la Caba, K. (2019). Citric acid-incorporated fish gelatin/chitosan composite films. *Food Hydrocolloids*, 86, 95-103.
Wang, D., Sun, J., Li, J., Sun, Z., Liu, F., Du, L., & Wang, D. (2022). Preparation and characterization of gelatin/zein nanofiber films loaded with perillaldehyde, thymol, or ε-polylysine and evaluation of their effects on the preservation of chilled chicken breast. *Food Chemistry*, 373, 131439.
Wang, D., Sun, Z., Sun, J., Liu, F., Du, L., & Wang, D. (2021). Preparation and characterization of polylactic acid nanofiber films loading Perilla essential oil for antibacterial packaging of chilled chicken. *International Journal of Biological*

Macromolecules, 192, 379-388.

Wang, W., Xiao, j., Chen, X., Luo, M., Liu, H., & Shao, P. (2018). Fabrication and characterization of multilayered kafirin/gelatin film with one-way water barrier property. *Food Hydrocolloids*, 81, 159-168.

Wu, W., Wu, Y., Lin, Y., & Shao, P. (2022). Facile fabrication of multifunctional citrus pectin aerogel fortified with cellulose nanofiber as controlled packaging of edible fungi. *Food Chemistry*, 374, 131763.

Xu, Y., Chu, Y., Feng, X., Gao, C., Wu, D., Cheng, W., Meng, L., Zhang, Y., & Tang, X. (2020). Effects of zein stabilized clove essential oil Pickering emulsion on the structure and properties of chitosan-based edible films. *International Journal of Biological Macromolecules*, 156, 111-119.

Yang, K., Liu, A., Hu, A., Li, J., Zen, Z., Liu, Y., Tang, S., & Li, C. (2021). Preparation and characterization of cinnamon essential oil nanocapsules and comparison of volatile components and antibacterial ability of cinnamon essential oil before and after encapsulation. *Food Control*, 123, 107783.

Zhang, L., Chen, D., Yu, D., Regenstein, J. M., Jiang, Q., Dong, J., Chen, W., & Xia, W. (2022a). Modulating physicochemical, antimicrobial and release properties of chitosan/zein bilayer films with curcumin/nisin-loaded pectin nanoparticles. *Food Hydrocolloids*, 133, 107955.

Zhang, S., He, Z., Xu, F., Cheng, Y., Waterhouse, G. I. N., Sun-Waterhouse, D., & Wu, P. (2022b). Enhancing the performance of konjac glucomannan films through incorporating zein–pectin nanoparticle-stabilized oregano essential oil Pickering emulsions. *Food Hydrocolloids*, 124, 107222.

Zhang, W., Jiang, H., Rhim, J. W., Cao, J., & Jiang, W. (2022c). Effective strategies of sustained release and retention enhancement of essential oils in active food packaging films/coatings. *Food Chemistry*, 367, 130671.

Zhang, W., Shu, C., Chen, Q., Cao, J., & Jiang, W. (2019). The multi-layer film system improved the release and retention properties of and its application as coating in inhibition to penicillium expansion of apple fruit. *Food Chemistry*, 299, 125109.

Zhao, G., Wang, S., Li, Y., Yang, L., & Song, H. (2023). Properties and microstructure of pickering emulsion synergistically stabilized by silica particles and soy hull polysaccharides. *Food Hydrocolloids*, 134, 108084.

Zhao, K., Wang, W., Teng, A., Zhang, K., Ma, Y., Duan, S., Li, S., & Guo, Y. (2020). Using cellulose nanofibers to reinforce polysaccharide films: Blending vs layer-by-layer casting. *Carbohydrate Polymers*, 227, 115264.

Zhao, R., Guan, W., Zhou, X., Lao, M., & Cai, L. (2022). The physiochemical and preservation properties of anthocyanidin/chitosan nanocomposite-based edible films containing cinnamon-perilla essential oil pickering nanoemulsions. *LWT-Food Science and Technology*, 153, 112506.

743 **Figure Caption**

744 **Fig. 1** Size distribution (A), Turbiscan stability index (B) and confocal laser scanning
745 microscopic (CLSM) images (C) of cinnamon essential oil (CEO) loaded (1%, v/v)
746 Pickering emulsion. The CLMS images (C) with 200 times magnification displayed
747 different observation status of CEO-loaded Pickering emulsion, including bright field
748 (i), the channel at 488 nm excitation wavelength (ii), the channel at 633 nm excitation
749 wavelength (iii) and stacked state of both 488nm and 633 nm channels (iv). CEO phase
750 (dyed by Nile Red) is denoted in red and the zein nanoparticle phase (dyed by Nile Blue)
751 is in green, respectively.

752 **Fig. 2** Scanning electron microscope (SEM) of different contents (0, 5, 7.5, and 10 mL)
753 cinnamon essential oil (CEO) loaded Pickering emulsion chitosan/gelatin composite
754 films with 300 times magnification. While CF represents blend casting chitosan/gelatin
755 films, BF represents bilayer assembly chitosan/gelatin films and the number represents
756 the CEO-loaded Pickering emulsion contents (0, 5, 7.5, and 10 mL) that be added to
757 films.

758 **Fig. 3** Appearance (A) and light transmittance (B1, B2) of different contents (0, 5, 7.5,
759 and 10 mL) cinnamon essential oil (CEO) loaded Pickering emulsion chitosan/gelatin
760 films. CF and BF represent blend casting and bilayer assembly chitosan/gelatin films,
761 and the number represents the CEO-loaded Pickering emulsion contents (0, 5, 7.5, and
762 10 mL) that be added to films.

763 **Fig. 4** FTIR (A), Wide-angle X-ray scattering (B), weight loss curves (C) and first order

764 derivative of weight loss curve (D) of different contents cinnamon essential oil (CEO)
765 loaded Pickering emulsion (5, 7.5 and 10 mL) in chitosan/gelatin films. CF and BF
766 represent blend casting and bilayer assembly chitosan/gelatin films, and the number
767 represents the CEO-loaded Pickering emulsion content (mL) that be added to films.

768 **Fig. 5** Water vapor permeability (WVP) and of different contents (0, 5, 7.5, and 10 mL)
769 cinnamon essential oil (CEO) loaded Pickering emulsion in blend casting
770 chitosan/gelatin films (A1) and bilayer assembly chitosan/gelatin films (A2). Oxygen
771 permeability (OP) of different contents (0, 5, 7.5, and 10 mL) cinnamon essential oil
772 (CEO) loaded Pickering emulsion in blend casting chitosan/gelatin films (B1) and
773 bilayer assembly chitosan/gelatin films (B2). Schematic diagram of water vapor and
774 oxygen through the blend casting and bilayer assembly of chitosan/gelatin films (C).
775 CF and BF represent blend casting and bilayer assembly chitosan/gelatin films, and the
776 number represents the CEO-loaded Pickering emulsion contents (0, 5, 7.5, and 10 mL)
777 that be added to films. Different superscripts within a column indicate significant
778 differences ($P < 0.05$).

779 **Fig. 6** The release behavior of cinnamon essential oil (CEO) in CEO-loaded Pickering
780 emulsion chitosan/gelatin films to different food simulants. 50% ethanol solution
781 simulated as semi-fatty foodstuffs (A1) and 95% ethanol solution simulated as fatty
782 foodstuffs (A2), respectively. Growth profiles of *P. paralactis* MN10 (B1) and *L.sakei*
783 VMR17 (B2) under treatment of different CEO-loaded Pickering emulsion
784 chitosan/gelatin films. And the morphology of *P. paralactis* MN10 and *L.sakei* VMR17

785 under different treatments by scanning electron microscope with 20000 times
786 magnification.

787 **Fig. 1**

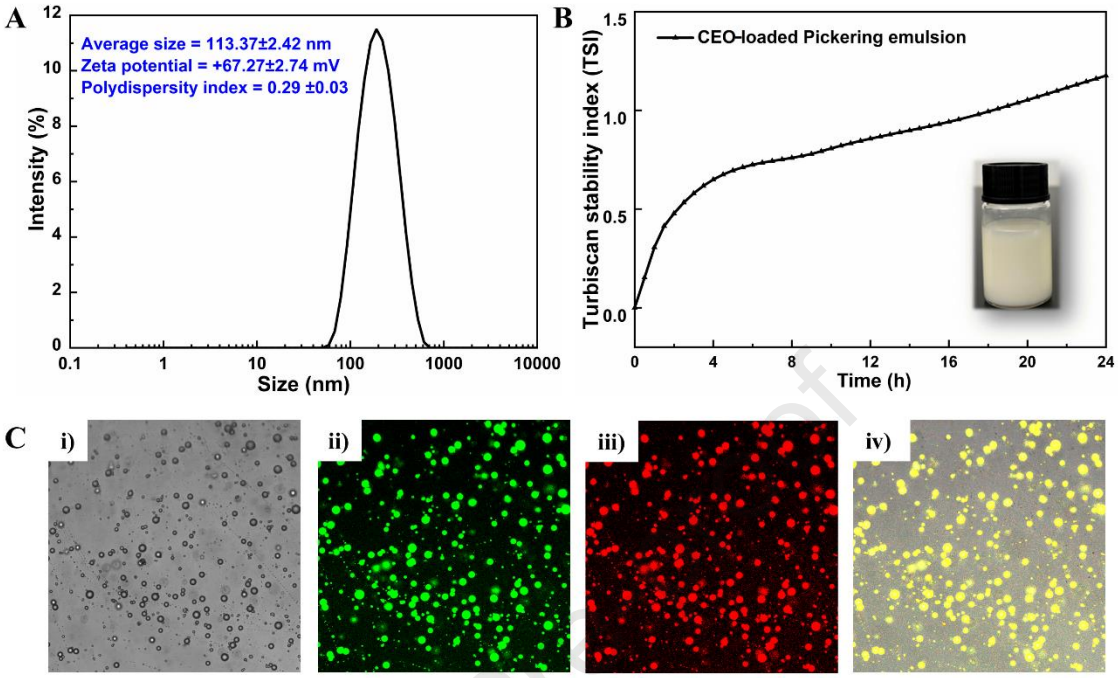

788

789 **Fig. 2**

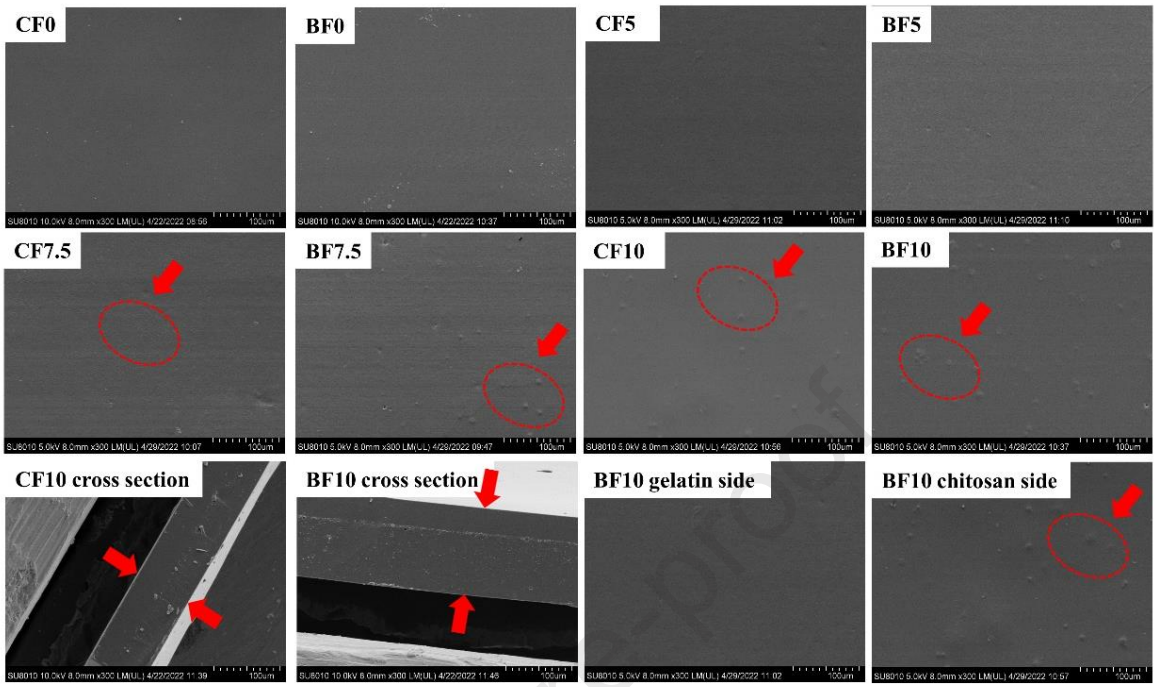

790

791 **Fig. 3**

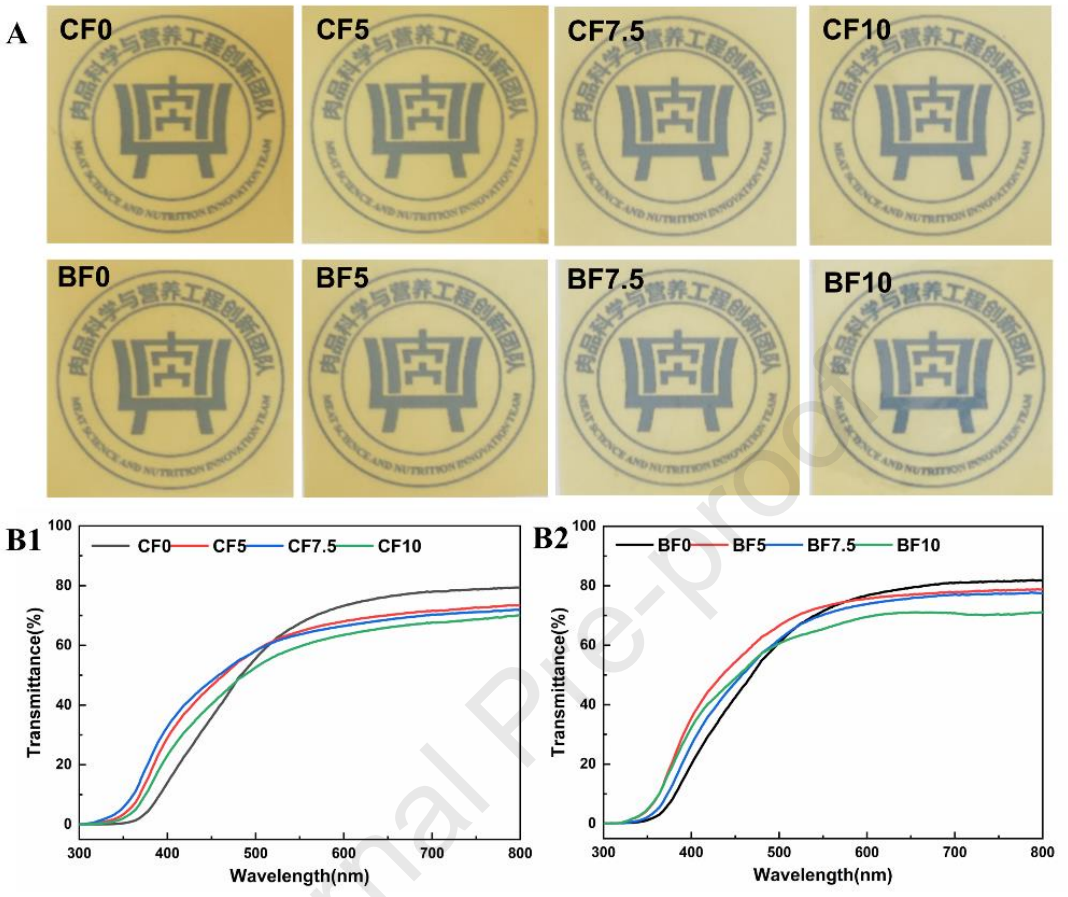

792

793 **Fig. 4**

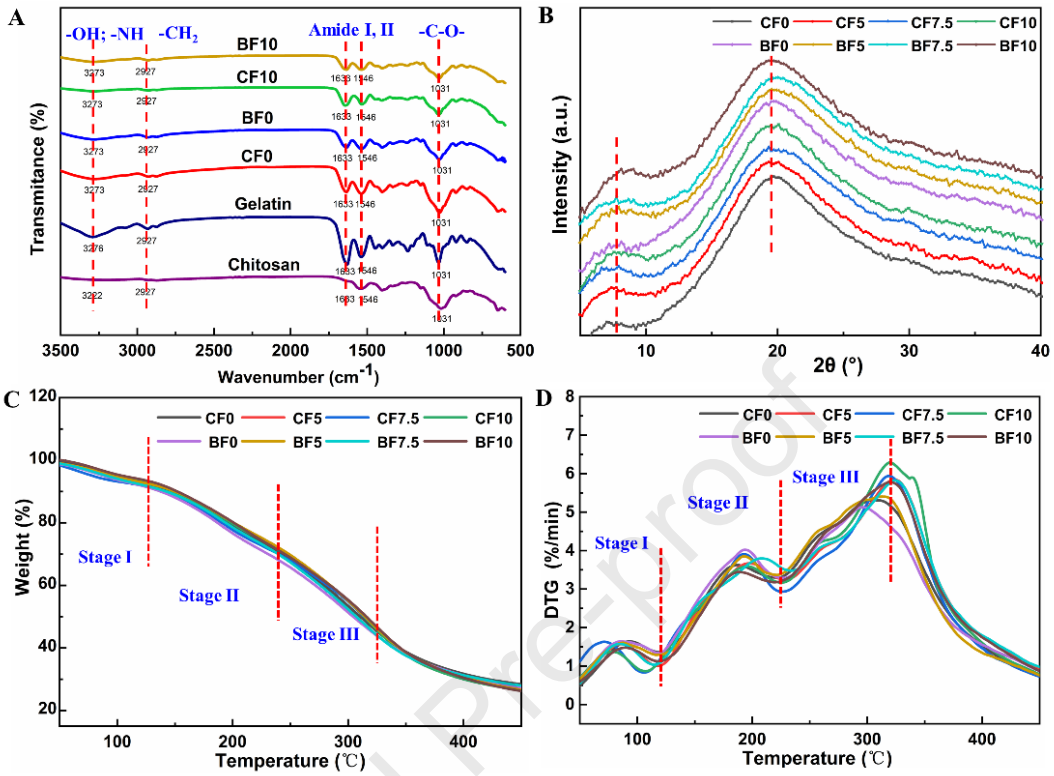

794

795 **Fig. 5**

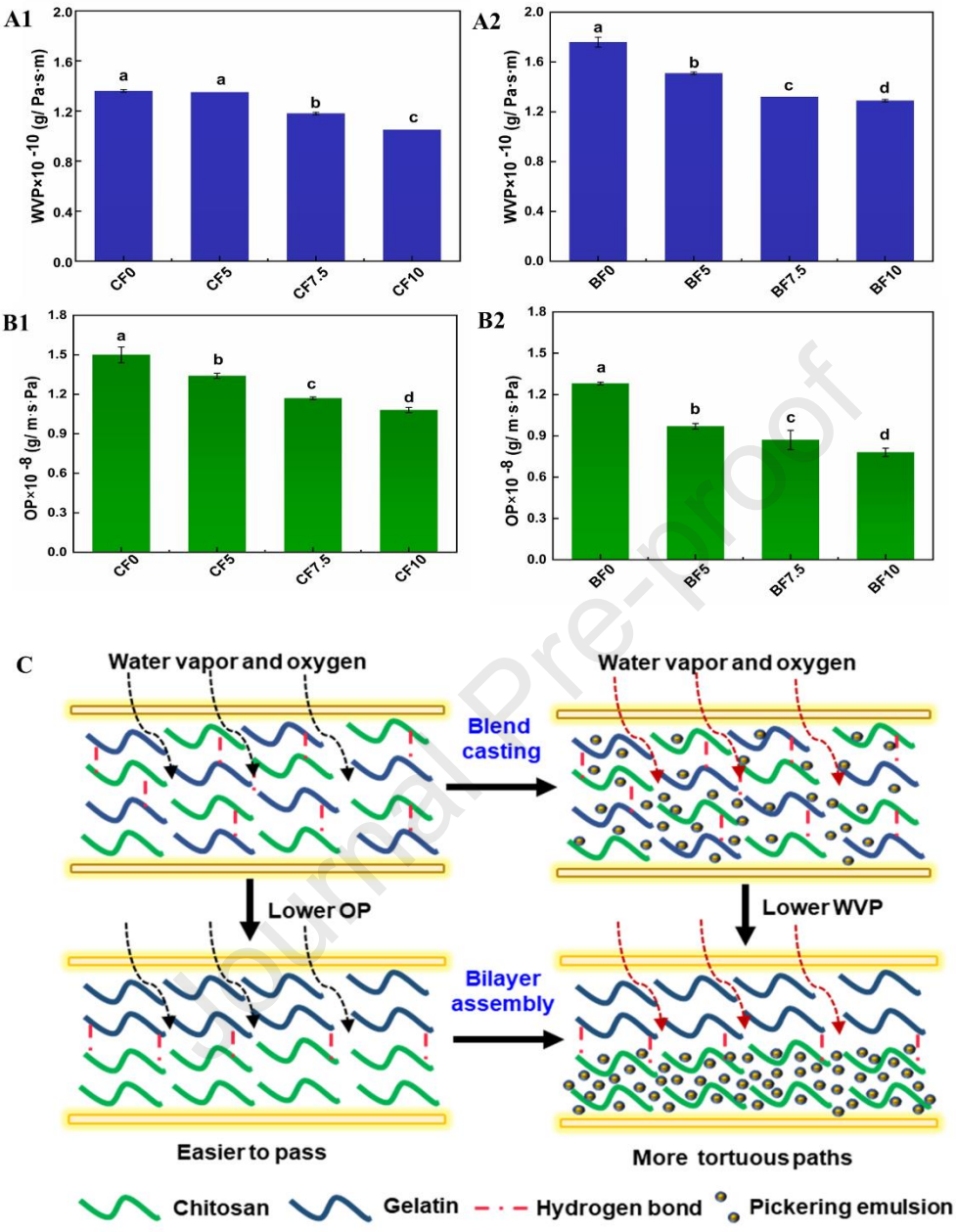
A1
WVP×10 -10 (g/ Pa·s·m)
a
a
b
c
CF0
CF5
CF7.5
CF10
A2
WVP×10 -10 (g/ Pa·s·m)
a
b
c
d
BF0
BF5
BF7.5
BF10
B1
OP×10 -8 (g/ m·s·Pa)
a
b
c
d
CF0
CF5
CF7.5
CF10
B2
OP×10 -8 (g/ m·s·Pa)
a
b
c
d
BF0
BF5
BF7.5
BF10
C
Water vapor and oxygen
Blend casting
Water vapor and oxygen
Lower OP
Lower WVP
Bilayer assembly
Easier to pass
More tortuous paths
Chitosan
Gelatin
Hydrogen bond
Pickering emulsion

796

797 **Fig. 6**

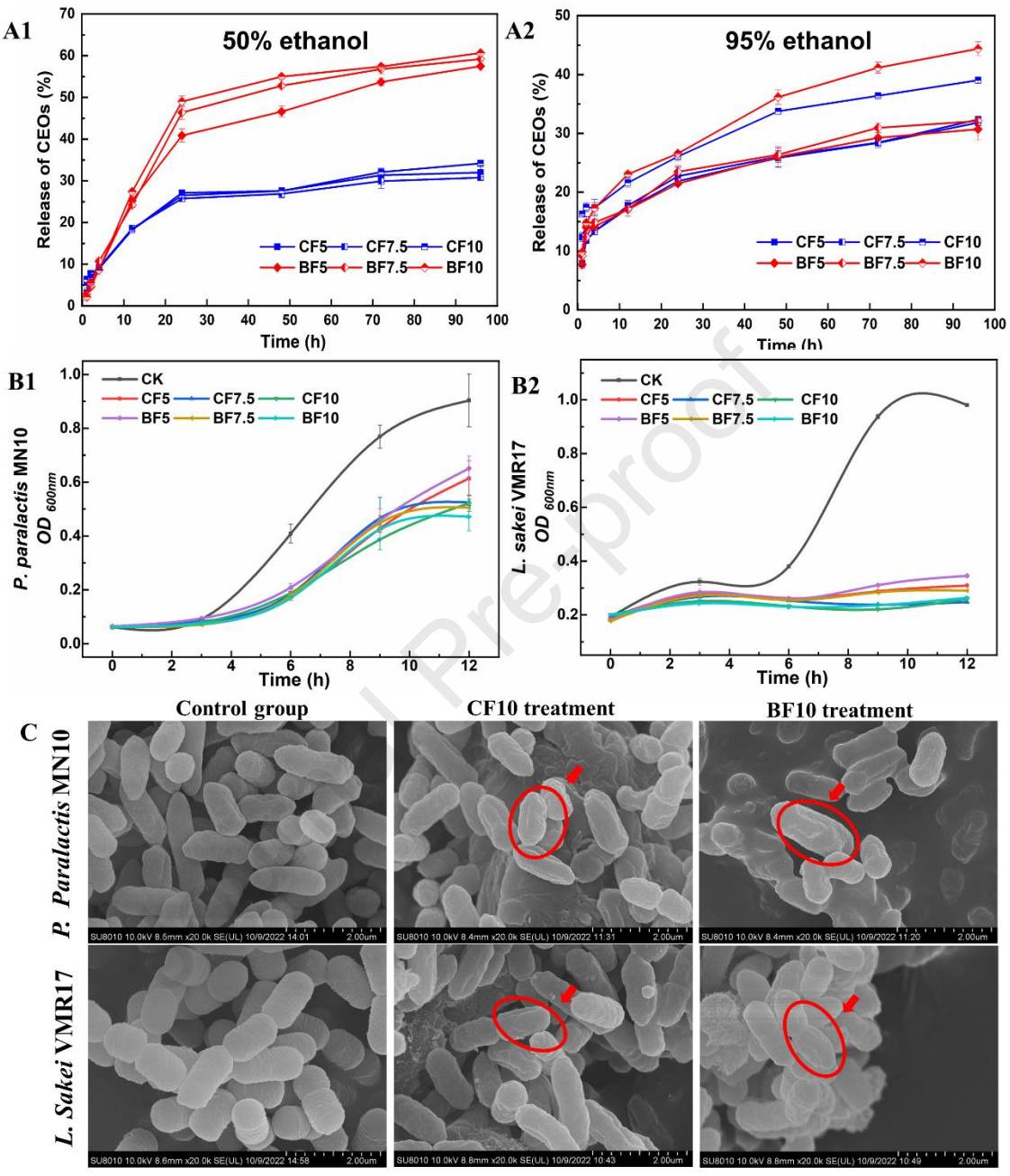
A1
50% ethanol
Release of CEOs (%)
Time (h)
CF5
CF7.5
CF10
BF5
BF7.5
BF10
A2
95% ethanol
Release of CEOs (%)
Time (h)
B1
P. paralactis MN10
OD 600nm
CK
CF5
CF7.5
CF10
BF5
BF7.5
BF10
Time (h)
B2
L. sakei VMR17
OD 600nm
Time (h)
C
Control group
CF10 treatment
BF10 treatment
P. Paralactis MN10
L. Sakei VMR17

798

799 **Table 1** Thickness, tensile strength (TS), elongation at break (EAB), water content

800 (WC), and water solubility (WS) of films.

Samples	Thickness (μm)	TS (MPa)	EAB (%)	WC (%)	WS (%)
CF0	66.61±4.27^{e}	12.96±0.98^{a}	3.95±0.50^{c}	28.04±0.26^{b}	41.38±0.48^{a}
CF5	67.52±3.61^{de}	9.91±1.06^{b}	5.17±0.06^{c}	24.07±0.26^{cd}	36.14±1.36^{b}
CF7.5	68.24±2.93^{de}	9.50±0.48^{b}	5.27±0.49^{c}	22.96±0.38^{d}	34.34±0.34^{bc}
CF10	74.81±3.34^{ab}	9.58±0.48^{b}	5.69±0.32^{c}	19.44±0.93^{e}	32.16±0.76^{bc}
BF0	69.85±2.86^{cde}	8.16±0.25^{c}	30.03±0.66^{b}	32.97±1.72^{ab}	35.86±0.14^{b}
BF5	70.24±1.83^{cd}	6.60±0.31^{de}	30.47±2.83^{ab}	29.23±2.18^{b}	33.06±1.48^{bc}
BF7.5	72.14±3.83^{bc}	6.35±0.56^{e}	32.31±1.86^{a}	27.30±0.62^{c}	30.50±2.84^{c}
BF10	78.03±4.07^{a}	6.58±0.25^{de}	33.63±1.16^{a}	20.94±0.94^{de}	29.26±1.99^{c}

801 Different superscripts in the same column indicate significant differences among films ($P < 0.05$).
802 CF and BF represent blend casting and bilayer assembly chitosan/gelatin films, and the number
803 represents the cinnamon-loaded Pickering emulsion contents (0, 5, 7.5, and 10mL) that be added
804 to films.

Highlights

- Pickering emulsion as antimicrobial agent delivery system.
- CEO-loaded Pickering emulsion was incorporated into CS/GEL complex films.
- Mechanical and barrier properties of prepared films were enhanced.
- The antimicrobial activities and control release behavior of films were shown.

Declaration of interests

☒ The authors declare that they have no known competing financial interests or personal relationships that could have appeared to influence the work reported in this paper.

☐ The authors declare the following financial interests/personal relationships which may be considered as potential competing interests: